IL-7 induces rapid clathrin-mediated internalization and JAK3-dependent degradation of IL-7Rα in T cells

Catarina M. Henriques[1], José Rino[2], Robert J. Nibbs[3], Gerry G. Graham[3], João T. Barata[1*]

[1] Cancer Biology Unit, [2] BioImaging Unit, Instituto de Medicina Molecular, Lisbon University Medical School, Lisbon, Portugal; [3] Division of Immunology, Infection & Inflammation, Glasgow Biomedical Research Centre, Glasgow, UK.

* Correspondence to: João T. Barata, Cancer Biology Unit, Instituto de Medicina Molecular, Lisbon University Medical School, Av. Prof. Egas Moniz, 1649-028 Lisboa, Portugal; Tel: +351217999524; Fax: +351217999524; e-mail: joao_barata@fm.ul.pt

Running title: IL-7Rα internalization, recycling and degradation

Word counts: 4427 (text) and 165 (abstract)

Number of Figures: 6

Number of References: 50

Scientific category: Immunobiology

Abstract

Interleukin 7 (IL-7) is an essential cytokine for T-cell development and homeostasis. It is well established that IL-7 promotes the transcriptional downregulation of *IL7RA* leading to decreased IL-7Rα surface expression. However, it is currently unknown whether IL-7 regulates the intracellular trafficking and early turnover of its receptor upon ligand binding. Here, we show that, in steady-state T-cells, IL-7Rα is slowly internalized and degraded, while a significant fraction recycles back to the surface. Upon IL-7 stimulation, there is rapid IL-7Rα endocytosis via clathrin-coated pits, decreased receptor recycling and accelerated lysosome and proteasome-dependent degradation. In accordance, the half-life of IL-7Rα decreases from 24h to approximately 3h after IL-7 treatment. Interestingly, we further demonstrate that clathrin-dependent endocytosis is necessary for efficient IL-7 signal transduction. In turn, pre-treatment of T-cells with JAK3 or pan-JAK inhibitors suggests that IL-7Rα degradation depends on the activation of the IL-7 signaling effector JAK3. Overall, our findings indicate that IL-7 triggers rapid IL-7Rα endocytosis, which is required for IL-7-mediated signaling and subsequent receptor degradation.

Introduction

Interleukin 7 (IL-7) is a key pro-survival cytokine essential for T-cell proliferation, development and homeostasis. IL-7 is produced by stromal cells in the thymus and bone marrow, and also by vascular endothelial cells, intestinal epithelium, keratinocytes and follicular dendritic cells[1]. The IL-7/ IL-7R signaling network was shown to be critical in health and disease. IL-7 is essential in lymphoid development, since knockout mice for IL-7 [2,3], IL-7Rα[4], γ_c[5], and JAK1[6] or JAK3[7] suffer similar lymphoid developmental blocks. IL-7 was also shown to rescue primary T-cell acute lymphoblastic leukemia (T-ALL) cells from spontaneous apoptosis *in vitro*[8] and IL-7 transgenic mice develop lymphomas[9]. Furthermore, IL-7 may be involved in chronic inflammation, osteoclast maturation and subsequent bone destruction in rheumatoid arthritis[10].

IL-7 signals via the IL-7 receptor, composed by the IL-7Rα and the gamma common chain (γ_c), which is shared by other interleukin receptors, namely IL-2, IL-4, IL-9, IL-15 and IL-21. Upon ligand binding, IL-7Rα and γ_c heterodimerize and are phosphorylated by JAK1/3[1]. In T-cells, this directs the activation of STAT5 and PI3K, leading to cell cycle progression, increased viability and cell size[1,8,11]. In general, effective signal transduction depends on the tight control of receptor membrane trafficking via internalization, degradation and recycling mechanisms[12], and may occur during receptor trafficking in intracellular vesicles, rather than just at the cell surface[13]. Moreover, endocytosis is commonly required for efficient receptor-mediated signal transduction, and it has been described for other cytokine receptors such as IL-2R[14] and IL-5R[15]. Receptor endocytosis can occur via clathrin-coated pits and/or clathrin-independent routes. For example, assembly of high affinity IL-2R and consequent signal transduction is dependent on lipid rafts[14]. Interestingly, the different chains of the receptor (α, β and γ_c) are differentially sorted after internalization: while β and γ_c

chains are targeted for degradation, the α chain internalizes constitutively and recycles back to the surface[16]. Other receptors, such as the IL-5R[15], TGFβ[17] and EGFR[18] internalize not only via clathrin-coated pits but also via clathrin-independent routes. Independently of the internalization route, it is thought that receptors traffic to early endosomes, where they can then be sorted for degradation and/or recycling[19,20]. Whether an internalized receptor is targeted for degradation or recycling depends on several factors, which differ between receptor and cell type [19]. Ubiquitination is usually associated with receptor degradation via proteasomes, but in some cases efficient degradation of ubiquitinated receptor relies on both proteasomes and lysosomes[21,22].

Dissecting how IL-7 regulates its cognate receptor membrane trafficking is crucial to the in-depth understanding of the role of IL-7/IL-7R in lymphocyte function. Previous studies have suggested that IL-7 stimulation of T-cells leads to surface down-modulation of IL-7Rα within 30 minutes, possibly due to receptor internalization[23]. At later time points (2-6h), IL-7 was shown to induce transcriptional downregulation of *IL7RA*[24-26]. However, the actual dynamics of IL-7Rα internalization and the regulation of trafficking mechanisms by IL-7 remain to be elucidated. In the present study, we show that IL-7 induces rapid clathrin-dependent IL-7Rα internalization in human T-cells. Moreover, our results suggest that IL-7-induced signaling is dependent on IL-7Rα internalization and that subsequent receptor degradation relies on JAK3 activity and is mediated by both proteasomes and lysosomes. Our study explores for the first time the mechanisms of IL-7-induced IL-7Rα trafficking, contributing to the understanding of the biology of the IL-7/IL-7R axis in lymphocyte function.

Materials & methods

Cell lines and primary human thymocytes. Human HPB-ALL cell line was cultured in RPMI-1640 (Gibco) supplemented with 10% (vol/vol) heat inactivated FBS (Gibco) and 2mM L-glutamine (hereafter referred to as RPMI-10). Cells were maintained at 37ºC in 5% CO2. Human thymocytes were isolated from thymic tissue obtained from children undergoing cardiac surgery. Samples were obtained with informed consent after institutional review board approval. The tissue was gently disrupted in RPMI and filtered through a cell strainer. Thymocytes were enriched by density centrifugation over Ficoll-Paque (GE Healthcare) to at least 95% purity.

Cell treatment with inhibitors. All cell culture experiments were performed in RPMI-10. When indicated, cells were pre-treated or not (vehicle control), with inhibitors at a density of 10^6 cells/mL, and inhibitors were kept during the duration of experiment: hyperosmotic sucrose (Sigma-Aldrich; 0.5M; 1h00 pretreatment), NH4Cl (Sigma-Aldrich; 50mM; 1h pretreatment), JAK3 inhibitor WHI-P131 (Calbiochem; 150μM; 1h pretreatment), pan-JAK inhibitor I (Calbiochem; 10 μM; 1h pretreatment), Cycloheximide (Sigma-Aldrich; 500 μM, 30min. pretreatment) Lactacystin (Calbiochem; 25μM, 1h pretreatment), Filipin (Sigma-Aldrich; 2.5μg/ml, 1h pretreatment)

Flow cytometry analysis. For cell surface assessment of receptor expression, cells were washed in ice cold PBS after the indicated stimulus/pre-treatment, resuspended in PBS/1% BSA (Sigma-Aldrich), and incubated for 30 min. on ice with α-human IL-7Rα- phycoerythrin (PE)-conjugated antibody (R&D), or isotype and concentration matched IgG-PE control. Cells were then washed in ice-cold PBS, resuspended in 2% paraformaldehyde (Sigma-

Aldrich), incubated 15 min. on ice, and analyzed using a FACScalibur flow cytometer (Becton Dickinson) and FlowJo software (TreeStar). For intracellular assessment of receptor expression, cells were washed in ice cold PBS after the indicated stimulus/pre-treatment, resuspended in 4% paraformaldehyde/0.05M sucrose and incubated at 4ºC for 15 min. After fixing, cells were washed in cold PBS as before, resuspended in 50mM NH4Cl in PBS for quenching, and incubated at room temperature for 10 min. After quenching, cells were washed with permeabilization buffer (PBS/1%BSA/0.05% saponin), resuspended in permeabilization buffer and incubated at 37ºC for 15 min. After incubation with antibody for 30 min at 37ºC, cells were washed in PBS, resuspended in 2% PFA, incubated for 15 min. on ice and analyzed by flow cytometry.

Antibody 'chase' for assessment of receptor co-localization. For confocal microscopy analysis, the HPB-ALL cell line was plated on PDL (Poly-D-lysine) (Sigma Aldrich)-coated coverslips for 30 min to 1h, at 37ºC for cells to adhere. To 'chase' the pool of surface receptor, cells were incubated in RPMI-10 for 30 min. on ice, with α-human IL-7Rα unconjugated antibody. After primary antibody labeling, cells are washed and resuspended in RPMI-10 and re-incubated on ice with α-IgG- Alexa 633 or 488 (Molecular Probes). After washing with PBS, cells were resuspended in RPMI-10 at the density of 10^6 cells/mL and stimulated or not (vehicle control) with recombinant human IL-7 (Peprotech) (50ng/ml) at 37ºC, for the indicated time intervals. After stimulation, cells were washed, fixed, quenched and permeabilized as for intracellular staining for flow cytometry analysis. Cells were then incubated for 1h at 37ºC in permeabilization buffer with antibodies for different endosomal compartments: clathrin heavy chain FITC-conjugated (Pharmingen); EEA1 FITC-conjugated (Pharmingen); LAMP2 Alexa Fluor 488-conjugated (Ebioscience); rabbit unconjugated Rab-11 (Zymed). When necessary, cells were washed in PBS and incubated with secondary

antibodies: when using FITC-coupled antibodies, α-FITC-Alexa Fluor 488-conjugated antibody (Molecular Probes) was used to enhance signal detection. For Rab-11 detection, we used α-rabbit-Alexa Fluor 488-conjugated antibody. After secondary incubation, cells were washed twice in permeabilization buffer and twice in PBS, followed by a 10 min incubation with 4% PFA/sucrose at 4ºC. Cells were washed again with PBS and slides were inverted over a drop of Vectashield/DAPI (Vector Laboratories) and sealed with varnish. Slides were analyzed by confocal microscopy, as detailed below. Image acquisition was performed with the pinhole aperture set to 1 Airy unit for the highest wavelength (633 nm) and adjusted for the lower wavelengths to maintain the same optical slice thickness for all channels. Five to ten different fields of view (~ 40 cells per field of view) were collected for quantification, which was performed for a given pair of fluorophores. The percentage of co-localizing cells was determined by counting the fraction of cells showing at least one co-localization event (minimum 3x3 pixels) between the fluorophores from live cells presenting both fluorophores only (cells in which only one of the fluorophores was present were discarded from the analysis).

Antibody feeding and recycling. The HPB-ALL cell line was plated onto PDL-coated coverslips as described for co-localization analysis. In parallel, 1M cells were plated on the different conditions coverslips. Initially all cells were incubated at 4ºC, in RPMI-10, with unconjugated α-human IL-7Rα antibody for 30 min. After this, cells are washed gently 3x with ice-cold PBS and transferred to 37ºC in the presence or absence of IL-7 (50ng/ml) for antibody feeding for 1h. Cells are subsequently washed again and the positive time zero control coverslip was further incubated at 4ºC with secondary α-mouse Alexa 488 antibody, in RPMI-10, for 30 min. Cells were fixed at the end with 2% PFA incubation for 15 min on ice and washed with PBS. The coverslip was then inverted onto a drop of Vectashield/DAPI

as described before. The negative control is obtained by performing an acid wash (RPMI-10 with Ph adjusted to 3), which removes all surface-bound antibody. After this acid wash, the primary antibody/receptor complex was allowed to recycle to the cell surface by switching the cells to 37ºC for the indicated time point, in pH 7 RPMI-10 (wash 2x with RPMI-10 after acid wash to re-establish normal pH). Recycling is stopped by washing the cells with cold PBS. Recycled IL-7Ra/unconjugated antibody complex is detected by incubating the cells with anti-mouse IgG Alexa 488 secondary antibody, for 30 minutes on ice. Slides were analyzed by confocal microscopy, as detailed below. Measurements of mean fluorescence intensity were performed with the pinhole set to its maximum aperture. This ensures that the fluorescence measured for each cell corresponds to the total surface intensity rather than a single optical slice. At least 8 different fields of view were imaged for each condition (~ 40 cells per field of view), keeping the same excitation (10% laser transmission) and detection settings throughout the acquisition. Image processing and quantification were performed with ImageJ (http://rsbweb.nih.gov.ij). Briefly, after being background subtracted, each image was thresholded to identify surface fluorescence signals whose mean intensity was then determined for each image. The threshold level was determined based on histogram analysis and was kept constant for each segmentation.

Confocal Microscopy. All images were acquired on a Zeiss LSM 510 META inverted confocal laser scanning microscope (Carl Zeiss, Jena, Germany) using a PlanApochromat 63x/1.4 oil immersion objective. DAPI fluorescence was detected with a violet 405 nm diode laser (30 mW nominal output) and a BP 420-480 filter. Both EGFP and Alexa Fluor 488 fluorescence were detected using the 488 nm laser line of an Ar laser (45 mW nominal output) and a BP 505-550 filter. Alexa Fluor 633 fluorescence was detected using a 633 nm HeNe laser (5 mW nominal output) and a custom META detector 636-754 band pass filter.

Transmitted light imaging was performed using one of the available laser lines and the transmitted PMT channel available in the LSM 510 META. Sequential multi-track/frame imaging sequences were used to avoid any potential bleed-through from the different fluorophores. All confocal images were acquired with a frame size of 512x512 pixels.

Time-Lapse Microscopy. For live time-lapse imaging, a procedure was used similar to the antibody chase technique and co-localization analysis. However, cells were kept alive throughout the procedure (no fixing or permeabilization). Cells were placed on ice until immediately before imaging, at which point they were transferred to the Zeiss LSM 510 META system equipped with an incubator chamber, where they were kept at a controlled 37ºC and 5% CO2 environment. Cells were either imaged unstimulated or after addition of IL-7 (50ng/ml). A total of 112 images were acquired with a time interval of 30 s between each image and 488 nm laser intensity set to 3% to minimize photobleaching. Images were background subtracted and further processed with ImageJ using a rigid body registration algorithm to correct for cell displacement during image acquisition. Movies of cells were then generated and time-annotated.

Immunoblotting. Following the indicated conditions and time intervals of culture, cell lysates were prepared, and equal amounts of protein (50μg/sample) were analysed by 12% sodium dodecyl sulphate–polyacrylamide gel electrophoresis (SDS-PAGE), transferred onto nitrocellulose membranes, and immunoblotted with the indicated antibodies. pJAK3 (Sigma-Aldrich); pSTAT5a/b (Upstate); pAKT (Cell Signaling); Actin and ZAP 70 (Upstate). After immunoblotting with antibodies, detection was performed by incubation with horseradish peroxidase-conjugated anti-mouse (Promega) or anti-rabbit (Promega) or anti-goat (Santa

Cruz) immunoglobulin (IgG, 1:5000 dilution), as indicated by the host origin of the primary antibody and developed by chemiluminescence.

Statistics. Data were analyzed using Graph Pad Prism software (San Diego, CA). Statistical analysis was performed using regular two-way ANOVA followed by Bonferroni post-tests when comparing unstimulated VS IL-7 internalization and degradation rates throughout time. When the unstimulated or IL-7-induced internalization or degradation was analyzed on its own, we used regular one-way ANOVA followed by Bonferroni post-tests. Student T-test was used to assess the effect of IL-7 with and without inhibitors, at a selected time point. Differences were considered with statistical significance for $p<0.05$.

Results

IL-7 induces rapid IL-7Rα internalization in T cells

To study the dynamics of IL-7Rα internalization we started by assessing cell surface expression over time, in the presence or absence of IL-7. Flow cytometry analysis showed that IL-7 induced rapid IL-7Rα surface downregulation, in normal human thymocytes (Supp. Figure 1) and in the T-ALL cell lines TAIL7 [27](data not shown) and HPB-ALL (Figure 1), which we used in subsequent experiments. Interestingly, we found that IL-7Rα surface levels decreased rapidly, with approximately 20% decrease upon 5 minutes, 30% after 15 minutes (Figure 1A) and 40% after 30 minutes of IL-7 stimulation (Figure 1A,B). This indicates that IL-7-mediated downregulation of IL-7Rα can occur more rapidly than previously suggested[23,25,26]. In addition, rapid IL-7-mediated IL-7Rα surface downregulation was dose-dependent and clearly observed at doses as low as 1ng/ml (Supp. Figure 2). To confirm that decreased surface expression was due to receptor internalization, we stained HPB-ALL cells with an unconjugated mouse anti-IL-7Rα antibody and an anti-mouse Alexa Fluor 488-conjugated secondary antibody on ice to label the IL-7Rα at the surface with minimal receptor internalization [28]. This strategy allowed us to follow the pool of surface receptor from a defined stimulation point onwards. Consistent with the flow cytometry data, the levels of surface receptor remained constant when cells were shifted to 37ºC in the absence of stimulus, whereas upon IL-7 stimulation there was clear receptor clustering and internalization (Fig 1 C and Supplementary video).

IL-7Rα internalization occurs via clathrin-coated pits and is required for IL-7-mediated signaling

Receptor-mediated endocytosis can occur via clathrin-coated pits and/or clathrin-independent routes, such as lipid rafts. Irrespectively of the internalization route, it is thought that internalized receptors traffic to an Early Endosome Antigen 1 (EEA-1)-positive early endosome, where they are sorted for degradation and/or recycling[12,19]. IL-2Rα, a cytokine receptor that shares γ_c with IL-7Rα, was shown to localize to lipid rafts and internalize in a lipid raft-dependent manner [14]. We therefore pre-treated the cells with Filipin, which is known to specifically inhibit lipid raft-dependent internalization[29] and assessed the impact on constitutive and IL-7-dependent IL-7Rα internalization. Our data suggest that the internalization of IL-7Rα is largely independent of lipid rafts (Supp. Figure 3).

IL-7 can induce phosphorylation of clathrin heavy chain in mouse T cell precursors [30], highlighting the potential involvement of clathrin in IL-7Rα internalization. To assess this hypothesis, we next analyzed the cellular localization of IL-7Rα, clathrin and EEA-1 by confocal microscopy, in the absence or presence of IL-7. We found that IL-7Rα constitutively co-localized with clathrin and with EEA-1 positive endosomes in 60.4% and 69.9% of the cells analyzed, respectively (Figure 2A). This suggests that IL-7Rα is internalized via clathrin-coated pits and traffics into early endosomes in a constitutive manner. Importantly, after 5 minutes of IL-7 stimulation, IL-7Rα co-localized with clathrin in 78.1% and with EEA-1 positive endosomes in 74.7% of the cells, suggesting that clathrin-dependent internalization into early endosomes rapidly increased in the presence of IL-7 (Figure 2A). To confirm these observations, we pre-treated the cells with hyperosmotic sucrose (0.5M), which has been shown to inhibit clathrin-dependent endocytosis[29]. IL-7-induced receptor internalization was abrogated by hyperosmotic sucrose pre-treatment (Figure 2B), indicating that endocytosis of IL-7Rα relies on clathrin-coated pits. Interestingly, inhibition of clathrin-mediated endocytosis blocked IL-7-induced signaling, as determined by phosphorylation of JAK1/JAK3, STAT5 and Akt/PKB (Fig 2C). These data show that, similarly to other

transmembrane receptors[15,18,31], clathrin-dependent endocytosis is required for effective triggering of IL-7-mediated signaling pathways, thereby underlining the functional relevance of IL-7Rα endocytosis via clathrin-coated pits.

A pool of internalized IL-7Rα constitutively recycles back to the cell surface

Although IL-7Rα constitutively internalized via clathrin-coated pits, the overall surface receptor levels were kept constant, and inhibition of clathrin-mediated endocytosis did not affect the surface receptor levels in the absence of IL-7 (data not shown). These observations raise the possibility that IL-7Rα may constitutively internalize and recycle back to the cell surface. To test this assumption, we assessed whether IL-7Rα co-localized with Rab-11-positive recycling endosomes[32]. We found that IL-7Rα co-localized with recycling endosomes both in the absence and presence of IL-7 stimulus, suggesting constitutive recycling of internalized receptor (Figure 3A). Next, we sought to quantify the amount of recycling IL-7Rα in both conditions. To do this, we performed an antibody feeding and recycling assay (adapted from Weber et al [33]), as described in 'Materials and Methods', in which the amount of antibody found at the surface corresponds to the amount of internalized and subsequently recycled IL-7Rα. The results confirmed that there is constitutive IL-7Rα recycling, which still occurs upon IL-7 stimulation, albeit somewhat less efficiently (Figure 3B,C). These data further indicate that there are no major differences in IL-7Rα recycling that could account for decreased surface expression upon IL-7 treatment.

IL-7 induces rapid IL-7Rα degradation in a proteasome and lysosome-dependent manner.

To further characterize the mechanisms involved in IL-7-mediated IL-7Rα surface downregulation, we next measured the total (surface plus intracellular) receptor levels by flow

cytometry. We observed rapid downregulation of IL-7Rα upon IL-7 stimulation (Figure 4A), which was consistent with immunoblot analysis (data not shown). In addition, pre-treatment of cells with the translation inhibitor cycloheximide revealed that the kinetics of IL-7Rα degradation was significantly accelerated upon IL-7 stimulation (Figure 4B). Accordingly, IL-7Rα half-life was dramatically decreased, from roughly 24 hours in unstimulated cells to around 3h in the presence of IL-7 (Figure 4B). These data indicate that IL-7-induced rapid IL-7Rα internalization was followed by significant receptor degradation.

Protein degradation is thought to occur via two main mechanisms in the cell, namely the ubiquitin-proteasome and the pH-dependent lysosomal degradation pathways[34]. To identify the routes of IL-7-induced IL-7Rα degradation, we pre-treated the cells with the specific proteasome inhibitor Lactacystin[35] or the lysosome inhibitor NH_4Cl, a lysomotropic agent[33,36], and evaluated total IL-7Rα expression. Our results show that NH_4Cl partially reversed, whereas Lactacystin completely prevented, IL-7-induced IL-7Rα degradation (Figure 4C). This suggests that both lysosomes and proteasomes participated in the degradation of the receptor. However, because NH_4Cl displayed only a partial effect, we sought to further demonstrate the involvement of lysosomes in the degradation of IL-7Rα. We performed receptor 'chase' and co-localization experiments using Alexa Fluor 633-labelled anti-IL7-Rα antibody and anti-LAMP-2 (Lysosome Associated Membrane Protein-2) Alexa Fluor 488-conjugated antibody to detect lysosomes[37]. As shown in figure 4D, we found that a significant portion of the receptor localized to lysosomes, after IL-7 stimulation (37% co-localizing cells in unstimulated conditions *vs*. 63% at 1h post-IL-7 simulation). These results suggest that, after IL-7 stimulation, a considerable fraction of the internalized IL-7Rα pool is degraded by lysosomes, probably in coordination with the ubiquitin-proteasome pathway. Thus, our data indicate that IL-7 induces IL-7Rα degradation by mechanisms that involve both proteasome and lysosome pathways.

IL-7-induced IL-7Rα degradation relies on JAK3 activity

The JAK family of tyrosine kinases has been previously implicated in the regulation of receptor trafficking[38,39]. In addition, IL-7 was shown to induce tyrosine phosphorylation of clathrin heavy chain, possibly via activation of JAK3 [30]. Therefore, we asked whether JAK kinases, and particularly JAK3, could be involved in IL-7Rα internalization and/or degradation. Pre-treatment of HPB-ALL cells with a JAK3-specific inhibitor[27] did not prevent IL-7Rα internalization, as determined by the analysis of IL-7Rα surface expression (Figure 5A,C). In contrast, JAK3 inhibition significantly reversed IL-7-induced IL-7Rα degradation (Figure 5B,C). Similar results were obtained using a pan-JAK inhibitor (Figure 5). Taken together, our data suggest that IL-7Rα degradation, but not internalization, is largely dependent on JAK3 activity.

Discussion

The generalized importance of IL-7 and its receptor for T-cell biology, with critical roles during development, homeostasis and differentiation, has raised particular interest on how IL-7Rα expression is regulated. It is currently established that IL-7, and other pro-survival cytokines, induce the transcriptional downregulation of *IL7RA* and consequently decrease significantly the cell surface expression of IL-7Rα at late time points (2-6h) [24-26]. This has been proposed as an altruistic mechanism for optimizing the access of T-cells to IL-7, which is expressed at limiting levels [26,40]. Here, we focused for the first time on the consequences of IL-7 stimulation regarding the early dynamics of IL-7Rα surface expression and associated mechanisms of internalization, recycling and degradation. We propose that on a steady state scenario, IL-7Rα at the cell surface takes part in a slow cycle of constitutive clathrin-dependent internalization and recycling, with a pool of receptor eventually being degraded and replaced by newly synthesized IL-7Rα. Upon IL-7 stimulation, endocytosis is rapidly accelerated and the balance is dramatically shifted towards degradation, in a manner that is dependent on JAK3 activation, which in turn appears to rely on IL-7Rα being internalized (Figure 6).

Previous work suggested that IL-7Rα is downregulated at the T-cell surface within 30 minutes of IL-7 stimulation, possibly due to internalization [23]. Alternatively, it has been proposed that IL-7 leads to IL-7Rα membrane shedding, instead of endocytosis [41]. However, this has been consistently challenged by recent studies [42-44]. In the present work, we describe for the first time the kinetics and mechanisms of IL-7Rα membrane trafficking in human T-cells, and confirm that IL-7 rapidly downregulates IL-7Rα surface levels. Importantly, both flow cytometry and confocal microscopy analyses revealed that IL-7Rα surface downregulation is mediated by clathrin-dependent internalization into early endosomes. This integrates well with previous observations that IL-7 induces phosphorylation of clathrin heavy

chain in mouse T-cells [30], which suggested that clathrin coated pits could be involved in IL-7Rα endocytosis. In agreement, we found that pre-treatment with sucrose-containing hypertonic media, which inhibits the formation of clathrin-coated pits[29], abrogated IL-7-induced IL-7Rα internalization.

Interestingly, we found that inhibition of clathrin-coated pits also largely prevented IL-7-mediated signaling, suggesting that IL-7Rα clathrin-dependent endocytosis is essential for optimal IL-7 signal transduction. This finding is not unprecedented. There is mounting evidence that endocytosis is frequently necessary for efficient receptor-mediated signal transduction [45]. From a complementary point of view, the ability to transduce a signal is also dependent on the availability of the receptor at the cell surface, which reflects the balance between *de novo* synthesis, internalization, degradation and recycling[46]. Our data suggest that IL-7Rα constitutively internalizes and either recycles back to the surface or is degraded in a process that is relatively slow – the half-life of the receptor is approximately 24h in non-stimulated cells. Since the expression of IL-7Rα at the cell surface of cultured T-cells is roughly constant, our observations implicate that, in steady state, *de novo* synthesis compensates for the pool of IL-7Rα that is slowly degraded. In the presence of IL-7, the route of IL-7Rα internalization remains clathrin-dependent. However, the kinetics is substantially accelerated and the receptor surface expression is reduced by more than 30% within only 15 minutes of stimulation. Although recycling still occurs, there is a major shift towards degradation. Consequently, the average half-life of IL-7Rα decreases dramatically to around 3h.

IL-7-induced receptor degradation appears to be mediated by both proteasomes and lysosomes. IL-7Rα co-localization with lysosomes is upregulated upon IL-7 stimulation, and pre-treatment with the lysomotropic agent NH_4Cl [36], which specifically inhibits pH-dependent lysosomal degradation[33], significantly downregulated IL-7Rα degradation. Additionally, the

proteasome inhibitor Lactacystin completely prevented IL-7Rα degradation. Lactacystin did not affect the internalization of the receptor (data not shown), suggesting that IL-7Rα internalization is independent of ubiquitin modification, in contrast to what has been described for some surface receptors[47]. There is evidence that the proteasome can play not only a direct role in proteolysis but also an indirect crucial function upstream of the lysosomal pathway, acting at the endosome level to sort proteins towards lysosome degradation[48,49]. Our observations that NH_4Cl and Lactacystin can both inhibit IL-7Rα degradation are in agreement with the hypothesis that the proteasome acts upstream of the lysosome in IL-7-mediated IL-7Rα proteolysis. The fact that Lactacystin is more effective may suggest that the proteasome is involved not only in sorting of activated receptor towards the lysosome but also directly in degradation. Alternatively, it is conceivable that NH_4Cl is not completely effective in inhibiting lysosomes, because it relies on a change in the pH to prevent lysosome protease activity. This could explain why we were not able to rescue IL-7Rα degradation as efficiently as by blocking an upstream step in the pathway.

Our present studies further indicate that activation of JAK3 is dispensable for IL-7-mediated receptor internalization, while playing a crucial role in IL-7Rα degradation. This is in line with IL-7 signaling, and therefore JAK3 activation, being evident only upon receptor endocytosis. Furthermore, since JAK3 associates with the γc, our data suggest the requirement of γc for efficient IL-7-mediated IL-7Rα degradation. Although we did not analyze the fate of γc after IL-7 stimulation, there is good evidence that IL-7Rα and γc co-localize. First, it is known that binding of IL-7Rα to γc is dependent on JAK3[50] Second, similarly to IL-7Rα, γc localizes to EEA-1 positive early endosomes and LAMP-1 positive lysosomes together with JAK3[38]. Notably, JAK3 is involved not only in triggering IL-7-mediated signaling but also in rapidly shutting it down by promoting the proteolysis of IL-7Rα. This indicates that the mechanisms of IL-7-dependent downregulation of IL-7Rα are not

restricted to, and can actually precede, the inhibition of *IL7RA* transcription [24-26]. The prevalence of these mechanisms is suggestive of the biological importance of limiting the surface expression of IL-7Rα in T-cells stimulated with IL-7, and may constitute further support to the 'altruistic model' [26,40]. Independently of these considerations, our data clarify how IL-7 stimulation impacts the trafficking of IL-7Rα in T-cells and thus may contribute to a more complete understanding of T lymphocyte biology and of diseases in which IL-7 and its receptor are thought to play a role, such as AIDS, multiple sclerosis, rheumathoid arthritis or leukemia.

Acknowledgements

This work was supported by IMM start-up funds and by the grant PTDC/SAU-OBD/104816/2008 from Fundação para a Ciência e a Tecnologia (to JTB). CMH has an FCT-SFRH PhD fellowship. We thank Dr. Miguel Abecasis for providing thymic samples.

Authorship contributions

C.M.H. designed research, performed all the experiments, analyzed and interpreted data, and wrote the manuscript; J.R. analyzed and interpreted data regarding microscopy experiments; R.J.N. and G.G.G. designed research, and analyzed and interpreted data; J.T.B. designed research, analyzed and interpreted data, and wrote the manuscript.

Disclosure of Conflicts of Interest

The authors have no conflict of interest to declare.

References

1. Jiang Q, Li WQ, Aiello FB, et al. Cell biology of IL-7, a key lymphotrophin. Cytokine Growth Factor Rev. 2005;16:513-533.
2. von Freeden-Jeffry U, Solvason N, Howard M, Murray R. The earliest T lineage-committed cells depend on IL-7 for Bcl-2 expression and normal cell cycle progression. Immunity. 1997;7:147-154.
3. von Freeden-Jeffry U, Vieira P, Lucian LA, McNeil T, Burdach SE, Murray R. Lymphopenia in interleukin (IL)-7 gene-deleted mice identifies IL-7 as a nonredundant cytokine. J Exp Med. 1995;181:1519-1526.
4. Peschon JJ, Morrissey PJ, Grabstein KH, et al. Early lymphocyte expansion is severely impaired in interleukin 7 receptor-deficient mice. J Exp Med. 1994;180:1955-1960.
5. Cao X, Shores EW, Hu-Li J, et al. Defective lymphoid development in mice lacking expression of the common cytokine receptor gamma chain. Immunity. 1995;2:223-238.
6. Rodig SJ, Meraz MA, White JM, et al. Disruption of the Jak1 gene demonstrates obligatory and nonredundant roles of the Jaks in cytokine-induced biologic responses. Cell. 1998;93:373-383.
7. Suzuki K, Nakajima H, Saito Y, Saito T, Leonard WJ, Iwamoto I. Janus kinase 3 (Jak3) is essential for common cytokine receptor gamma chain (gamma(c))-dependent signaling: comparative analysis of gamma(c), Jak3, and gamma(c) and Jak3 double-deficient mice. Int Immunol. 2000;12:123-132.
8. Barata JT, Cardoso AA, Boussiotis VA. Interleukin-7 in T-cell acute lymphoblastic leukemia: an extrinsic factor supporting leukemogenesis? Leuk Lymphoma. 2005;46:483-495.
9. Rich BE, Campos-Torres J, Tepper RI, Moreadith RW, Leder P. Cutaneous lymphoproliferation and lymphomas in interleukin 7 transgenic mice. J Exp Med. 1993;177:305-316.
10. Churchman SM, Ponchel F. Interleukin-7 in rheumatoid arthritis. Rheumatology (Oxford). 2008;47:753-759.
11. Barata JT, Silva A, Brandao JG, Nadler LM, Cardoso AA, Boussiotis VA. Activation of PI3K is indispensable for interleukin 7-mediated viability, proliferation, glucose use, and growth of T cell acute lymphoblastic leukemia cells. J Exp Med. 2004;200:659-669.
12. Le Roy C, Wrana JL. Clathrin- and non-clathrin-mediated endocytic regulation of cell signalling. Nat Rev Mol Cell Biol. 2005;6:112-126.
13. Hoeller D, Volarevic S, Dikic I. Compartmentalization of growth factor receptor signalling. Curr Opin Cell Biol. 2005;17:107-111.
14. Matko J, Bodnar A, Vereb G, et al. GPI-microdomains (membrane rafts) and signaling of the multi-chain interleukin-2 receptor in human lymphoma/leukemia T cell lines. Eur J Biochem. 2002;269:1199-1208.
15. Lei JT, Martinez-Moczygemba M. Separate endocytic pathways regulate IL-5 receptor internalization and signaling. J Leukoc Biol. 2008;84:499-509.
16. Hemar A, Subtil A, Lieb M, Morelon E, Hellio R, Dautry-Varsat A. Endocytosis of interleukin 2 receptors in human T lymphocytes: distinct intracellular localization and fate of the receptor alpha, beta, and gamma chains. J Cell Biol. 1995;129:55-64.
17. Di Guglielmo GM, Le Roy C, Goodfellow AF, Wrana JL. Distinct endocytic pathways regulate TGF-beta receptor signalling and turnover. Nat Cell Biol. 2003;5:410-421.
18. Sigismund S, Argenzio E, Tosoni D, Cavallaro E, Polo S, Di Fiore PP. Clathrin-mediated internalization is essential for sustained EGFR signaling but dispensable for degradation. Dev Cell. 2008;15:209-219.

19. Gonzalez-Gaitan M. The garden of forking paths: recycling, signaling, and degradation. Dev Cell. 2008;15:172-174.
20. Perrais D, Merrifield CJ. Dynamics of endocytic vesicle creation. Dev Cell. 2005;9:581-592.
21. Walrafen P, Verdier F, Kadri Z, Chretien S, Lacombe C, Mayeux P. Both proteasomes and lysosomes degrade the activated erythropoietin receptor. Blood. 2005;105:600-608.
22. van Kerkhof P, Strous GJ. The ubiquitin-proteasome pathway regulates lysosomal degradation of the growth hormone receptor and its ligand. Biochem Soc Trans. 2001;29:488-493.
23. Swainson L, Verhoeyen E, Cosset FL, Taylor N. IL-7R alpha gene expression is inversely correlated with cell cycle progression in IL-7-stimulated T lymphocytes. J Immunol. 2006;176:6702-6708.
24. Kim HR, Hwang KA, Kim KC, Kang I. Down-regulation of IL-7Ralpha expression in human T cells via DNA methylation. J Immunol. 2007;178:5473-5479.
25. Alves NL, van Leeuwen EM, Derks IA, van Lier RA. Differential regulation of human IL-7 receptor alpha expression by IL-7 and TCR signaling. J Immunol. 2008;180:5201-5210.
26. Park JH, Yu Q, Erman B, et al. Suppression of IL7Ralpha transcription by IL-7 and other prosurvival cytokines: a novel mechanism for maximizing IL-7-dependent T cell survival. Immunity. 2004;21:289-302.
27. Barata JT, Boussiotis VA, Yunes JA, et al. IL-7-dependent human leukemia T-cell line as a valuable tool for drug discovery in T-ALL. Blood. 2004;103:1891-1900.
28. Willingham IPaMC ed Endocytosis. Plenum Press, NY; 1985.
29. Ivanov AI. Pharmacological inhibition of endocytic pathways: is it specific enough to be useful? Methods Mol Biol. 2008;440:15-33.
30. Jiang Q, Benbernou N, Chertov O, Khaled AR, Wooters J, Durum SK. IL-7 induces tyrosine phosphorylation of clathrin heavy chain. Cell Signal. 2004;16:281-286.
31. Mills IG. The interplay between clathrin-coated vesicles and cell signalling. Semin Cell Dev Biol. 2007;18:459-470.
32. Horgan CP, Oleksy A, Zhdanov AV, et al. Rab11-FIP3 is critical for the structural integrity of the endosomal recycling compartment. Traffic. 2007;8:414-430.
33. Weber M, Blair E, Simpson CV, et al. The chemokine receptor D6 constitutively traffics to and from the cell surface to internalize and degrade chemokines. Mol Biol Cell. 2004;15:2492-2508.
34. Ciechanover A. Intracellular protein degradation from a vague idea through the lysosome and the ubiquitin-proteasome system and on to human diseases and drug targeting: Nobel Lecture, December 8, 2004. Ann N Y Acad Sci. 2007;1116:1-28.
35. Dick LR, Cruikshank AA, Grenier L, Melandri FD, Nunes SL, Stein RL. Mechanistic studies on the inactivation of the proteasome by lactacystin: a central role for clasto-lactacystin beta-lactone. J Biol Chem. 1996;271:7273-7276.
36. Houdebine LM, Djiane J. Effects of lysomotropic agents, and of microfilament- and microtubule-disrupting drugs on the activation of casein-gene expression by prolactin in the mammary gland. Mol Cell Endocrinol. 1980;17:1-15.
37. Eskelinen EL, Tanaka Y, Saftig P. At the acidic edge: emerging functions for lysosomal membrane proteins. Trends Cell Biol. 2003;13:137-145.
38. Hofmann SR, Lam AQ, Frank S, et al. Jak3-independent trafficking of the common gamma chain receptor subunit: chaperone function of Jaks revisited. Mol Cell Biol. 2004;24:5039-5049.
39. Martinez-Moczygemba M, Huston DP, Lei JT. JAK kinases control IL-5 receptor ubiquitination, degradation, and internalization. J Leukoc Biol. 2007;81:1137-1148.

40. Mazzucchelli R, Durum SK. Interleukin-7 receptor expression: intelligent design. Nat Rev Immunol. 2007;7:144-154.
41. Vranjkovic A, Crawley AM, Gee K, Kumar A, Angel JB. IL-7 decreases IL-7 receptor alpha (CD127) expression and induces the shedding of CD127 by human CD8+ T cells. Int Immunol. 2007;19:1329-1339.
42. Blom-Potar MC, Bugault F, Lambotte O, Delfraissy JF, Theze J. Soluble IL-7Ralpha (sCD127) and measurement of IL-7 in the plasma of HIV patients. J Acquir Immune Defic Syndr. 2009;51:104-105.
43. Rose T, Lambotte O, Pallier C, Delfraissy JF, Colle JH. Identification and biochemical characterization of human plasma soluble IL-7R: lower concentrations in HIV-1-infected patients. J Immunol. 2009;182:7389-7397.
44. Faucher S, Crawley AM, Decker W, et al. Development of a quantitative bead capture assay for soluble IL-7 receptor alpha in human plasma. PLoS One. 2009;4:e6690.
45. Sorkin A, von Zastrow M. Endocytosis and signalling: intertwining molecular networks. Nat Rev Mol Cell Biol. 2009;10:609-622.
46. Zi Z, Klipp E. Steady state analysis of signal response in receptor trafficking networks. Genome Inform. 2007;18:100-108.
47. Yu A, Malek TR. The proteasome regulates receptor-mediated endocytosis of interleukin-2. J Biol Chem. 2001;276:381-385.
48. Rocca A, Lamaze C, Subtil A, Dautry-Varsat A. Involvement of the ubiquitin/proteasome system in sorting of the interleukin 2 receptor beta chain to late endocytic compartments. Mol Biol Cell. 2001;12:1293-1301.
49. Alwan HA, van Zoelen EJ, van Leeuwen JE. Ligand-induced lysosomal epidermal growth factor receptor (EGFR) degradation is preceded by proteasome-dependent EGFR de-ubiquitination. J Biol Chem. 2003;278:35781-35790.
50. Page TH, Lali FV, Groome N, Foxwell BM. Association of the common gamma-chain with the human IL-7 receptor is modulated by T cell activation. J Immunol. 1997;158:5727-5735.

Figure Legends

Figure 1. IL-7 induces rapid IL-7Rα surface downregulation due to receptor internalization. (A) HPB-ALL cells were cultured in the presence or absence of IL-7 (50ng/ml) in culture medium for the indicated time points and subsequently analyzed by flow cytometry for surface IL-7Rα expression, as described in 'Materials and Methods'. Relative IL-7Rα expression was calculated as the geometric mean intensity of fluorescence normalized to the time zero control. Data represent mean±sem from at three independent experiments. * $P<0.05$, *** $P<0.001$ (One-way ANOVA, with Bonferroni's post-test). **(B)** Representative flow cytometry histogram overlay of IL-7Rα surface expression in HPB-ALL cells stimulated for 30 minutes with IL-7 (gray line) or left unstimulated (black line). **(C)** IL-7Rα internalization visualized by time-lapse microscopy of HPB-ALL cells. IL-7Rα initially expressed at the cell surface, was stained with α-human IL-7Rα unconjugated antibody, subsequently re-incubated with a secondary α-mouse IgG-Alexa488-conjugated antibody, and imaged for the indicated time points, with or without addition of IL-7 (50ng/ml), as described in the 'Materials and Methods'. See supplementary data for full time-lapse microscopy video. Representative cells of each condition from two independent experiments are shown.

Figure 2. IL-7Rα internalization via clathrin-coated pits and trafficking into early endosomes is required for efficient IL-7-mediated signaling. **(A)** Analysis of IL-7Rα co-localization with clathrin and EEA1 was performed by confocal microscopy. HPB-ALL cells were plated on PDL-coated coverslips, incubated at 4ºC with α -human IL-7Rα unconjugated antibody, and subsequently with a secondary α-mouse IgG-Alexa-633 antibody (red). Cells were then shifted to 37ºC in the presence or absence of IL-7 (50ng/ml) for 5 min, fixed, quenched and permeabilized. Endosomal compartments were detected using FITC-conjugated

antibodies for clathrin heavy-chain or EEA1, both enhanced by α-FITC-Alexa Fluor 488 secondary antibody (green). The two bottom images are 3D projections and include DAPI-stained nuclei. Representative cells of three independent experiments are shown. The percentage of co-localizing cells is indicated and was determined by counting the fraction of cells showing at least one co-localization event between red and green fluorescence. **(B)** HPB-ALL cells were pretreated or not with 0.5M sucrose (hypertonic media) for 1h, to inhibit formation of clathrin-coated pits, and then stimulated with 50ng/ml IL-7 or left untreated for 30 min. IL-7Rα surface expression was analyzed by flow cytometry and relative expression was calculated by normalizing the geometrical mean of fluorescence of the cell population in the presence of IL-7 stimulus, divided by the unstimulated condition at the same time point (30 min). Data represent mean±sem from three independent experiments: * $P<0.05$. **(C)** HPB-ALL cells were pretreated or not with 0.5M sucrose, and stimulated with 50ng/ml IL-7 for 30 min. Immunoblotting was performed and IL-7 mediated signaling assessed by detection of phosphorylated JAK1/3, STAT5a/b and AKT. ZAP-70 was used as a loading control.

Figure 3. A pool of internalized IL-7Rα recycles to the cell surface. (A) Co-localization between IL-7Rα and Rab-11 recycling endosomes was assessed after 5 min of stimulation with IL-7 (50ng/ml). Total IL-7Rα expression was assessed by intracellular staining as for flow cytometry. Rab-11 positive vesicles were further detected by incubation with rabbit α-human Rab-11 unconjugated antibody followed by secondary detection with α -rabbit IgG Alexa 488. Coverslips were mounted over Vectashield /DAPI. Cells representative of three independent experiments are shown. **(B)** Co-localization between IL-7Rα and endosomes was performed by antibody chase and co-localization assay, as described in Materials & Methods. Briefly, all cells, plated onto coverslips, were initially incubated at 4ºC with unconjugated α-human IL-7Rα antibody for 30 min and subsequently washed and transferred to 37ºC in the presence

or absence of IL-7 (50ng/ml) for 1h to allow for IL-7Rα internalization. Cells were washed and the positive control (time zero) was generated by incubating the cells at 4ºC with α-mouse IgG Alexa 488 secondary antibody for 30 min. The remaining coverslips underwent an acid wash treatment to remove surface-bound antibody. The negative control was not further processed. The primary antibody/receptor complex was allowed to recycle to the cell surface in the experimental conditions, by switching the cells to 37ºC again for 1h. Recycled IL-7Rα/antibody complex was detected by incubating the cells with anti-mouse IgG Alexa 488 secondary antibody for 30 minutes on ice. Cells were fixed and the different coverslips mounted with Vectashield/DAPI. Representative images of two independent experiments are shown for each condition. **(C)** Microscopy images of the antibody feeding and recycling assays were quantified by determining the Mean Intensity of Fluorescence (MIF) of at least 8 independent fields of view for each condition. ** P<0.01, *** P<0.001 (Students t-test, two-tailed).

Figure 4. IL-7 stimulation accelerates IL-7Rα degradation, in a lysosome and proteasome-dependent manner. (A,B,C) Total IL-7Rα expression (surface plus intracellular) was assessed by flow cytometry analysis of fixed and permeabilized HPB-ALL cells. Analysis of the data was performed as described in Figure 1. * P<0.05, ** P<0.01, *** P<0.001 (One-way ANOVA, with Bonferroni's post-test). **(B)** To determine IL-7Rα half-life cells were treated with the translation inhibitor cycloheximide (CHX). **(C)** To determine the pathways of degradation of IL-7Rα, cells were pre-treated for 1h with 50mM NH_4Cl or 25μM Lactacystin, and then stimulated or not with 50ng/ml IL-7 for 1h. The geometrical mean of fluorescence of the population was determined by flow cytometry, as shown in the representative histogram. * P<0.05 (Student T-test, two-tailed). Data in A, B and C represent mean±sem from at least three independent experiments. **(D)** Co-localization between IL-7Rα

and lysosomes in the presence or absence of IL-7 (1h; 50ng/ml) was performed using α-human IL-7Rα antibody and LAMP-2 as a lysosome marker. The percentage of co-localizing cells is indicated and was determined as in Figure 2. Representative cells of three independent experiments are shown.

Figure 5. IL-7-induced IL-7Rα degradation, but not internalization is JAK3 dependent. (A,B) Surface (A) and total (B) IL-7Rα expression in HPB-ALL cells was assessed as described by flow cytometry. Cells were pre-treated with 150μM of JAK3 inhibitor (WHI-P131) or PAN-JAK inhibitor I, and then stimulated or not with IL-7 (50ng/ml) for 30 min (A) or 1h (B). The geometrical mean of fluorescence for each population was determined by flow cytometry. Data (mean±sem) are from three independent experiments. * $P<0.05$ (Student T-test, two-tailed). **(C,D)** Representative flow cytometry histogram overlay of surface (C) or total (D) IL-7Rα expression in HPB-ALL cells pre-treated (black line) or not (gray line) with the JAK3 inhibitor WHI-P131, followed by IL-7 stimulation for 30 min (C) or 1h (D).

Figure 6. Proposed model for IL-7Rα trafficking. At the steady state, IL-7Rα is slowly internalized via clathrin-coated pits and recycled back to the cell surface, with a pool of receptor being degraded and replaced by newly synthesized IL-7Rα (not shown). Upon IL-7 stimulation, the balance is rapidly shifted towards receptor endocytosis and subsequent degradation. JAK3 activation, which appears to rely on IL-7Rα being internalized, is critical for triggering receptor degradation.

FIGURE 1

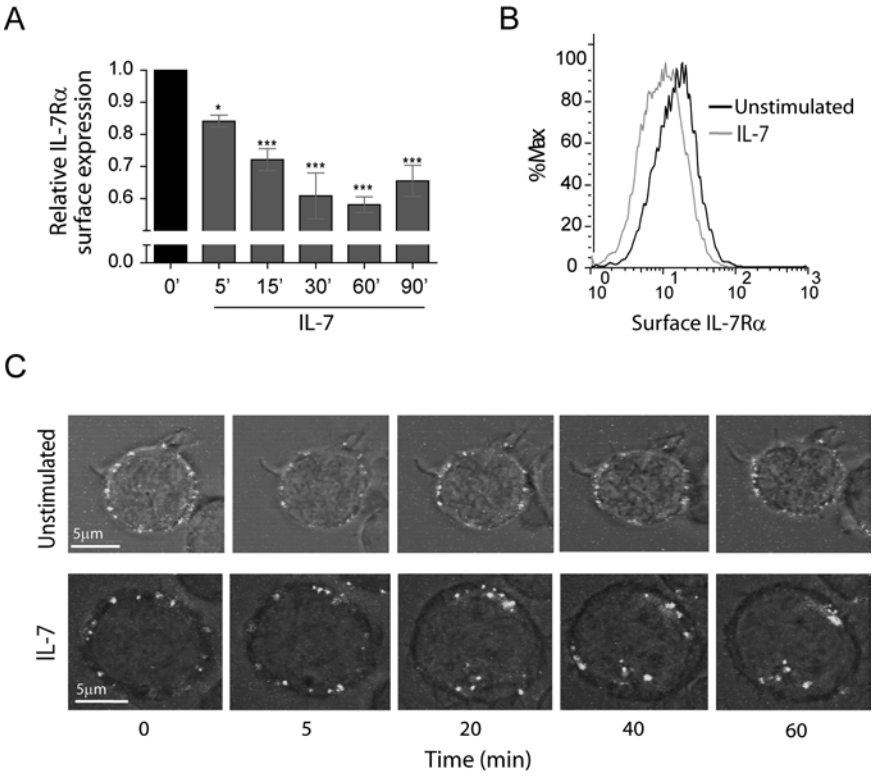
A
Relative IL-7Rα surface expression
1.0
0.9
0.8
0.7
0.6
0.0
*
***
***
***
***
0'
5'
15'
30'
60'
90'
IL-7
B
%Max
100
80
60
40
20
0
Unstimulated
IL-7
Surface IL-7Rα
C
Unstimulated
IL-7
5μm
5μm
0
5
20
40
60
Time (min)

FIGURE 2

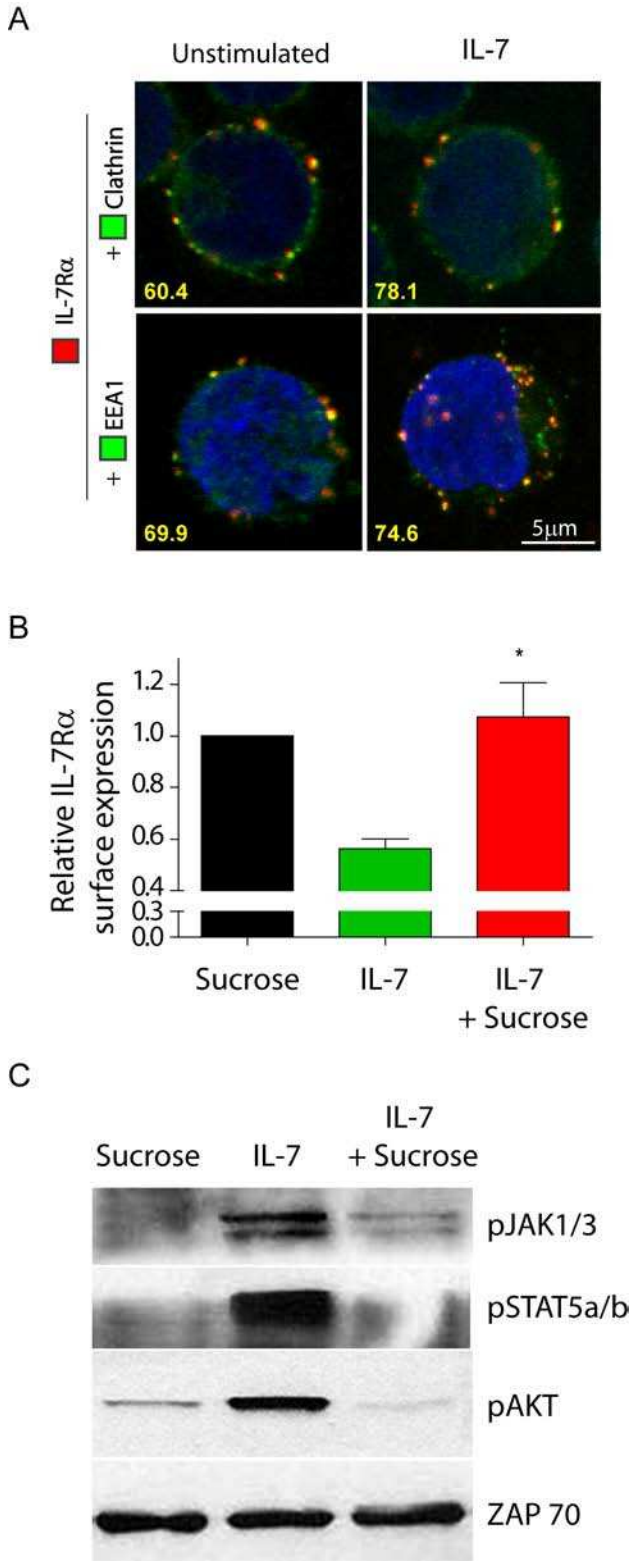
A
Unstimulated
IL-7
IL-7Rα
+ Clathrin
+ EEA1
60.4
78.1
69.9
74.6
5μm
B
Relative IL-7Rα surface expression
1.2
1.0
0.8
0.6
0.4
0.3
0.0
*
Sucrose
IL-7
IL-7 + Sucrose
C
Sucrose
IL-7
IL-7 + Sucrose
pJAK1/3
pSTAT5a/b
pAKT
ZAP 70

FIGURE 3

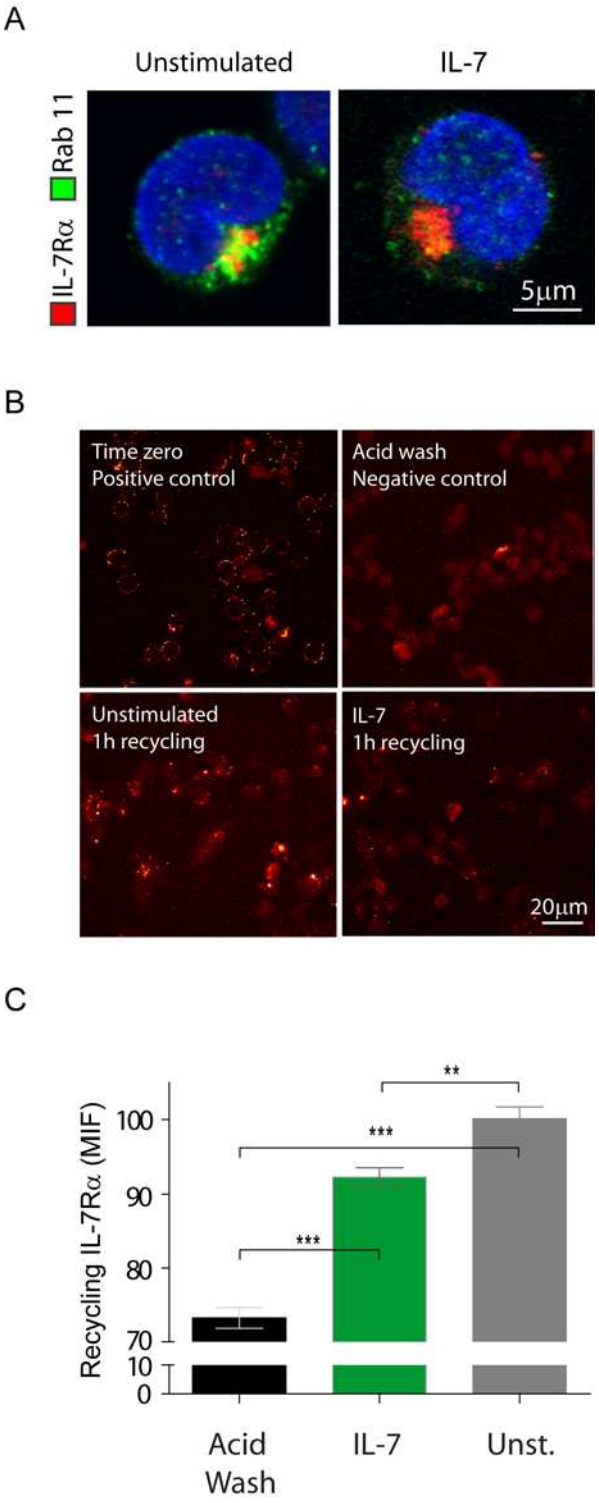
A
Unstimulated
IL-7
Rab 11
IL-7Rα
5μm
B
Time zero
Positive control
Acid wash
Negative control
Unstimulated
1h recycling
IL-7
1h recycling
20μm
C
Recycling IL-7Rα (MIF)
100
90
80
70
10
0
**
***
***
Acid
Wash
IL-7
Unst.

FIGURE 4

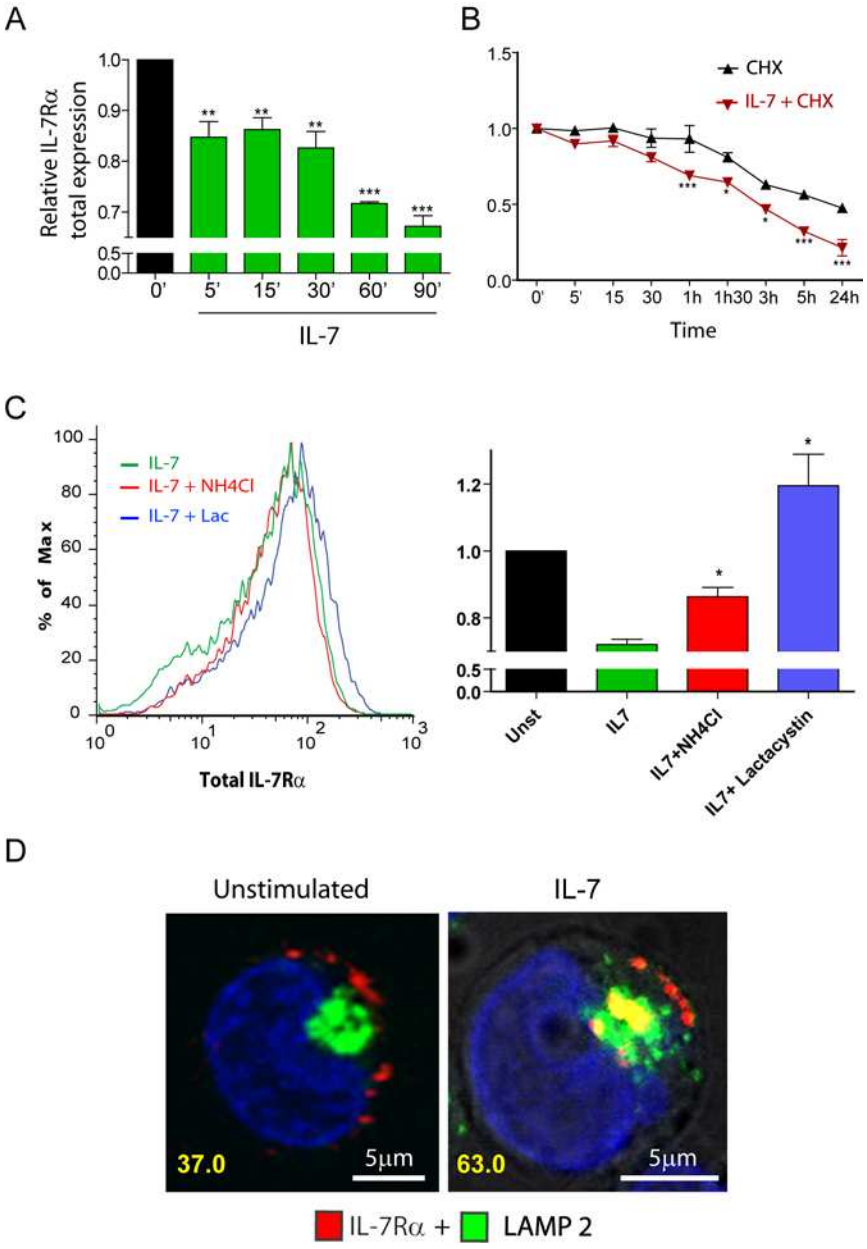
A
Relative IL-7Rα total expression
1.0
0.9
0.8
0.7
0.5
0.0
0'
5'
15'
30'
60'
90'
IL-7
B
CHX
IL-7 + CHX
1.5
1.0
0.5
0.0
0'
5'
15
30
1h
1h30
3h
5h
24h
Time
C
IL-7
IL-7 + NH4Cl
IL-7 + Lac
% of Max
100
80
60
40
20
0
Total IL-7Rα
Unst
IL7
IL7+NH4Cl
IL7+ Lactacystin
D
Unstimulated
IL-7
37.0
63.0
5µm
IL-7Rα + LAMP 2

FIGURE 5

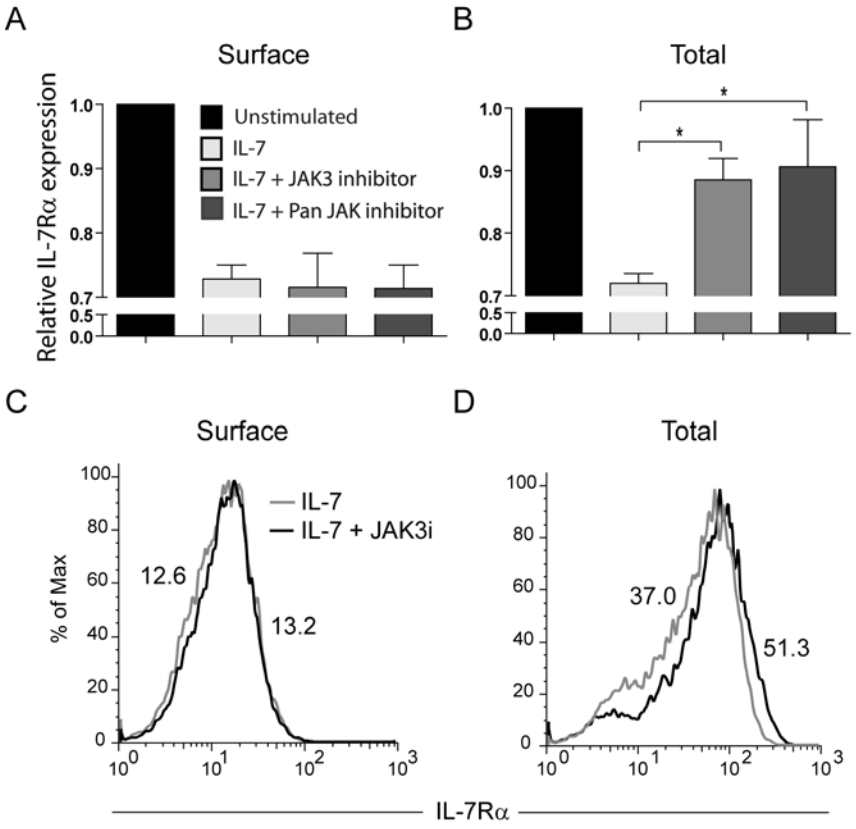
A
Surface
Relative IL-7Rα expression
1.0
0.9
0.8
0.7
0.5
0.0
Unstimulated
IL-7
IL-7 + JAK3 inhibitor
IL-7 + Pan JAK inhibitor
B
Total
*
*
C
Surface
% of Max
IL-7
IL-7 + JAK3i
12.6
13.2
D
Total
37.0
51.3
IL-7Rα

FIGURE 6

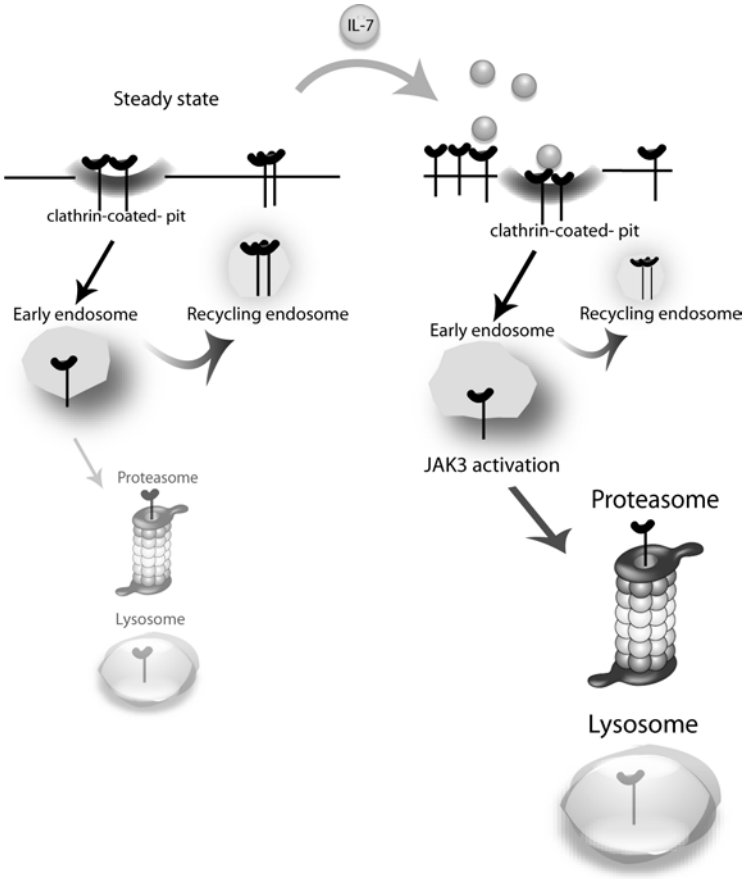
IL-7
Steady state
clathrin-coated- pit
Early endosome
Recycling endosome
Proteasome
Lysosome
clathrin-coated- pit
Early endosome
Recycling endosome
JAK3 activation
Proteasome
Lysosome